hep-ph/9508267

MSU-HEP/50808

REVISED

Improving the Measurement of the Top Quark Mass

Jon Pumplin

Department of Physics & Astronomy

Michigan State University

East Lansing, MI

Internet address: pumplin@msupa.msu.edu

(February 1, 2008)

Abstract

Two possible ways to improve the mass resolution for observing hadronic top quark decay $t \to bW \to 3\,\text{jets}$ are studied: (1) using fixed cones in the rest frames of the t and W to define the decay jets, instead of the traditional cones in the rest frame of the detector; and (2) using the jet angles in the top rest frame to measure m_t/m_W. By Monte Carlo simulation, the second method is found to give a useful improvement in the mass resolution. It can be combined with the usual invariant mass method to get an even better mass measurement. The improved resolution can be used to make a more accurate determination of the top quark mass, and to improve the discrimination between $t\bar{t}$ events and background for studies of the production mechanism.

I. INTRODUCTION

The discovery of the top quark in $p\bar{p}$ collisions [1,2] was a milestone for the Standard Model. The next steps beyond that milestone will be to improve the measurement of the top mass, and to test our understanding of QCD further by studying the details of its production and decay.

We focus here on the "single-lepton" channel defined by $p\bar{p} \to t\bar{t}X$ with one top decaying hadronically ($t \to W^+ b \to 3\,\text{jets}$, or its charge conjugate) and the other decaying leptonically ($t \to W^+ b \to \ell^+ \nu_\ell + 1\,\text{jet}$, or its charge conjugate, with $\ell = e$ or μ). This channel is experimentally favorable because the high $p_\perp$ lepton and large missing $p_\perp$ due to the neutrino provide a clean event signature that naturally discriminates against backgrounds. We will concentrate on the hadronically decaying top, since the treatment of the leptonically decaying one is complicated by errors in the measurement of the transverse momentum of the neutrino, via missing $p_\perp$, and by ambiguity in its longitudinal momentum.

We will not deal here with the question of how $t\bar{t}$ events are to be identified [1–3]. Rather we will concentrate on the problem of measuring m_t once the events have been isolated. The mass determination relies on measuring the energies and directions of jets, and inferring from them the energies and directions of the original quarks. In addition to instrumental calibrations, this requires corrections for the hard-scale branching of partons, and for non-perturbative hadronization effects. These hard and soft QCD effects can be modeled by event generators such as HERWIG [4], which have been shown to describe the appropriate physics in Z^0 decay at the e^+e^- collider LEP [5,6], where the original $q\bar{q}$ energy is precisely known.

Part of the top quark analysis involves measuring the mass of the hadronically decaying W boson. An eventual goal of the analysis should be to confirm the QCD effects in W decay that are similar to those seen in great detail for Z^0 decay. In the meantime, we can assume that the QCD effects are understood, and use the W mass for help in determining the correct jet assignments in $t\bar{t}$ events. The decay $W \to 2\,\text{jets}$ is also a potentially useful tool

to calibrate the detector, since the decay jets probe the detector at a wide range of angles and jet transverse momenta, and the W mass is accurately known [7]. This calibration is unavailable outside of top quark events, because hadronic W decays are generally obscured by large QCD backgrounds [8].

We will investigate two ideas that might improve the mass resolution. The first idea, examined in Sect. II, is to use fixed cones in the rest frames of the decaying t and W to define the jets, in place of the usual cones defined in the rest frame of the detector. The second idea, examined in Sect. III, is to use the angles between jets in the t rest frame to measure m_t/m_W directly.

II. REST FRAME CONE METHOD

The first idea that we will investigate can be understood most clearly by considering the W mass measurement. Since the W is color neutral, its decay products have nothing to do with other jets present in the final state. In the rest frame of the W, the decays will look very similar to the Z^0 decays studied at LEP. They will almost always appear as back-to-back jets that can be defined by two fixed cones of half-angle θ_0 oriented in opposite directions. Reasonable cone sizes are on the order of $\theta_0 = 45°$. Cones of this size are large enough to contain a good fraction of the energies of the jets, which are broadened by the collinear radiation singularity of QCD; while they are small enough to leave a large fraction $\cos\theta_0$ of the full 4π of solid angle outside the two cones, so not too much "background" is included in them. Although cone algorithms are not the traditional jet definitions in e^+e^- physics, they have been shown to work there, and even to provide superior resolution in jet angle and energy [6].

This proposal to try fixed cones in the W rest frame is quite different from the current experimental procedure for top analysis, where jets are defined by cones $\sqrt{(\Delta\eta)^2 + (\Delta\phi)^2} < R$ in the Lego variables of the detector. Those variables, $\eta = -\log\tan\theta/2 =$ pseudorapidity and $\phi =$ azimuthal angle, are Lorentz invariant only under boosts along the beam direction.

Meanwhile, the W can have a rather large component of boost transverse to the beam. For example, in $t\bar{t}$ events with typical acceptance cuts, the middle 60% of the W transverse momentum distribution extends from 40 GeV/c to 110 GeV/c, so $p_\perp^W$ is not small compared to m_W. Lego-defined jet cones therefore correspond to a wide variety of sizes and shapes of "cone" in the W rest frame, depending on the boost and hence depending on details that have nothing to do with the W decay.

Similarly, the jet cone for the b-quark jet from $t \to W\,b$ is most reasonably defined by a fixed angle in the t rest frame. Since the b carries color, the argument for a cylindrically symmetric cone in this frame is weaker than in the case of the W decay. But the t rest frame is nevertheless at least more logical than using the rest frame of the detector.

It would similarly be reasonable to define the jet cone for the other b-jet, from the semileptonically decaying top, in the rest frame of that top. That should be done when this method is applied to real data. But we ignore it for the moment, in order to avoid bringing in the issue of how to estimate the longitudinal momentum of the neutrino, which is needed to find that frame.

The idea of using fixed cones in the decay rest frames to define the jets is easy to implement as a follow-on to the traditional top quark analysis with "kinematic reconstruction" [1], *i.e.*, with explicit matching of the observed jets to decay partons. The procedure for each event is:

1. Identify the four-momenta of the jets corresponding to $t \to j_1\,j_2\,j_3$ and $t \to j_4\ell\nu$, where j_1, j_2 come from W decay and j_3, j_4 are b-quark jets, by the usual procedures of CDF or DØ. b-jet tagging is helpful for this, but not essential. There may of course be additional jets observed in the event.

2. Define j_F and j_B to be four-momenta directed in the forward and backward beam directions: $j_F = (1; 0, 0, 1)$ and $j_B = (1; 0, 0, -1)$ for beams in the z-direction.

3. Redefine the 4-momentum of j_1 as the sum of the 4-momenta observed in the calorimeter detector in all cells ("towers") that lie within θ_0 of the old j_1 in the rest frame of

the old $j_1 + j_2$. However, do not include cells that lie closer in angle to j_2, j_3, j_4, j_F, or j_B than to j_1.

Similarly redefine the 4-momentum of j_2 as the sum of the 4-momenta of all cells that lie within θ_0 of the old j_2 in the rest frame of the old $j_1 + j_2$, and are not closer in angle to j_1, j_3, j_4, j_F, or j_B.

Similarly redefine the 4-momentum of j_3 as the sum of the 4-momenta in cells that lie within θ_0 of the old j_3 in the rest frame of the old $j_1 + j_2 + j_3$, and are not closer in angle to j_1, j_2, j_4, j_F, or j_B.

4. Replace the old jet 4-momentum estimates by the new ones and repeat Step 3 a few times. This iteration converges completely for $> 99.8\%$ of events. A maximum of 10 iterations is sufficient, since the momenta stop changing before that for $> 99.5\%$ of events.

The major new work is in Step 3, which is very easy to implement in the following way. Treat the energy in every cell of the detector that receives energy above its noise level as if it came from a zero-mass particle. There will typically be a few hundred such cells in each event. Make a list of their four-momenta. The appropriate elements of this list to be added in the various parts of Step 3 can be found without making explicit Lorentz transformations, using the exact formula for the angle θ between $\vec{p}$ and $\vec{q}$ in the rest frame of r

$$\cos\theta = \frac{p{\cdot}r\, q{\cdot}r - p{\cdot}q\, r^2}{\sqrt{[(p{\cdot}r)^2 - p^2\, r^2]\,[(q{\cdot}r)^2 - q^2\, r^2]}}\,, \tag{1}$$

which holds for any four-vectors p, q, r.

To test the idea, HERWIG 5.7 [4] was used to simulate the single-leptonic top channel at the Tevatron energy $\sqrt{s} = 1.8\,\mathrm{TeV}$. Typical experimental cuts were approximated by $|\eta^\ell| < 2.0$, $p_\perp^\ell > 20\,\mathrm{GeV/c}$, $p_\perp^\nu > 25\,\mathrm{GeV/c}$. The four hadron jets were required, at the partonic level, to have $p_\perp^{\mathrm{jet}} > 20\,\mathrm{GeV/c}$ and to be isolated in Lego from the lepton by $\sqrt{(\Delta\eta)^2 + (\Delta\phi)^2} > 0.5$ and from each other by $\sqrt{(\Delta\eta)^2 + (\Delta\phi)^2} > 0.8$. The detector was simulated by an array of 0.1×0.1 cells in (η, ϕ), covering the region $-4.5 < \eta < 4.5$. Gaussian energy resolutions

with $\Delta E/E = 0.55/\sqrt{E}$ for charged hadrons and $\Delta E/E = 0.15/\sqrt{E}$ for leptons and photons were assumed (in GeV = 1 units). A small amount of shower spreading was also included: the energy of each final hadron was spread over a disk of radius 0.1 in the (η, ϕ) plane, before being deposited in the appropriate calorimeter cells.

A cone-type jet finding algorithm described previously [9] was used to search for jets in the simulated calorimeter. A small cone size $R = 0.3$ was used, as is standard practice in top quark analysis (CDF uses $R = 0.4$) to reduce the loss of events from overlapping jets, since one is asking for 4 jets within a rather small area in Lego — *e.g.*, all four decay jets lie within some strip of width 2.0 in η in 62% of the events. A minimum observed jet $p_\perp$ of 15 GeV/c was required. A feature of my jet-finder [9] is that it finishes with an iteration in which each cell of the detector that lies within R of at least one jet axis is assigned to the nearest jet axis. The jet momenta are then recomputed and this procedure is repeated. This feature tends to improve the mass resolution for objects decaying into jets. It is similar to the procedure being tried here, except that the nearest jets are now to be defined by angles in the appropriate rest frames.

To obtain a sample that could be cleanly interpreted, the "observed" jets in the simulation were matched to their original quark partons, using a criterion based on the agreement in Lego variables η and ϕ, along with a contribution from the agreement in $p_\perp$. A good match was obtained for 85% of the events, upon which Fig. 1 and Fig. 2 are based.

Fig. 1 shows the histogram of the mass observed for $W \to$ jj. The *dotted curve* is for jets defined by $\sqrt{(\Delta\eta)^2 + (\Delta\phi)^2} < R = 0.3$ in the Lego variables of the detector. Note that the center of the peak is well below the actual $m_W = 82\,\mathrm{GeV/c^2}$ assumed in the simulation, and that the peak is very asymmetrical, with a tail toward lower jj masses. This skewing of the mass distribution toward low mass is a direct result of gluon radiation falling outside the cone, which is characteristic of QCD, and which has been verified at LEP. It demonstrates that making QCD corrections is a very important part of the top quark mass measurement, especially if a cone size as small as 0.3 is used.

The *solid curve* in Fig. 1 shows the result of redefining the jets using a larger cone size $R = 0.7$. This included an iteration in which each calorimeter cell that lies within R of at least one of the 3 jet axes from hadronic t decay is reassigned to the jet with the nearest of those axes. This iteration is crucial to obtaining the improvement in mass resolution shown. Note that the qualitative QCD feature of skewing toward lower mass is still visible, but much less pronounced. Also, the center of the peak is at a higher mass, closer to the true partonic mass.

The cone size $R = 0.7$ is about optimal. If the width of the mass peak is defined by the range ΔM that contains the middle 50% of the probability distribution, then $\Delta M/M$ goes from 0.197 to 0.151 to 0.133 as R is increased from 0.3 to 0.5 to 0.7.

The *dashed curve* in Fig. 1 shows the result of redefining the jets in the appropriate decay rest frames by the steps enumerated above. The curve shown is for $\theta_0 = 45°$, which is about optimal. One sees that the mass resolution obtained this way is quite good ($\Delta M/M = 0.138$), but not as good as the $R = 0.7$ curve.[1]

Fig. 2 shows a similar histogram of the mass observed for $t \to W\,b \to \mathrm{jjj}$. One again sees QCD skewing of the peak toward lower masses, relative to the value $m_t = 175\,\mathrm{GeV/c^2}$ assumed in the simulation. This mass shift includes a contribution of $\approx -4\,\mathrm{GeV/c^2}$ from losses in observed jet energy due to neutrinos. One again sees a dramatic reduction in skewing and improvement in the resolution, when the cone size is increased from $R = 0.3$ (*dotted curve*) to $R = 0.7$ (*solid curve*). We emphasize that to obtain this improvement, it

[1] An early version of this paper claimed that defining jet cones in these "appropriate" rest frames led to superior mass resolution. The improvement found actually resulted from the fact that the rest-frame cones were on average larger than the Lego cones used there, in concert with the iterations in which each calorimeter cell is associated with the nearest jet axis. As long as such iterations are included, conventional Lego cones of size $R \simeq 0.7$ provide as good or slightly better resolution, as shown here.

is essential to use the iterative procedure whereby each calorimeter cell is assigned to the nearest decay jet axis.

The cone size $R = 0.7$ is again about optimal. Defining as before the width of the peak by the range ΔM that contains the middle 50% of the probability distribution, $\Delta M/M$ goes from 0.186 to 0.149 to 0.125 as R is increased from 0.3 to 0.5 to 0.7 .

The suggestion to define the jets using a fixed cone angle in the rest frame of the t for the b-jet, and in the rest frame of the W for its decay jets, which was proposed in this section, leads to the *dashed curve* in Fig. 2. One sees that, as in Fig. 1, this plausible idea does not in fact improve the mass resolution ($\Delta M/M = 0.130$), compared to $R = 0.7$ cones — although it is not much worse, either.

III. JET ANGLE METHOD

So far, we have computed the observed masses of t and W directly from the 4-momenta of the jets into which they decay, as simply the invariant mass of the sum of those jet momenta. The estimated 4-momentum of each jet is obtained by adding the 4-momenta detected by the calorimeter cells inside its jet cone. The t and W are thus formally treated as decaying into a large number of zero-mass particles that represent the energies deposited in the detector. Defined in this way, the individual jets have sizeable invariant masses — often on the order of $10\,\mathrm{GeV/c^2}$ or higher.

A possible alternative method to determine the top mass in each event would be to use only the *directions* of the jets in the top rest frame, treating the jets as zero-mass objects. To do this, let ψ_1 and ψ_2 be the angles between the b-jet and the two jets from W decay in that frame. Then $\psi_3 = 2\pi - \psi_1 - \psi_2$ is the angle between the W decay jets. According to zero-mass kinematics,

$$\frac{m_t}{m_W} = \frac{\sin\psi_1 \,+\, \sin\psi_2 \,+\, \sin\psi_3}{\sqrt{2\,\sin\psi_1\,\sin\psi_2\,(1-\cos\psi_3)}}\,. \tag{2}$$

The angles needed in this formula can be obtained from the measured jet 4-momenta in any frame using Eq. (1). At the partonic level, the use of zero-mass kinematics is promising

since, *e.g.*, the energy of the b-quark is $\approx 70\,\mathrm{GeV}$, so the influence of its mass $m_b \approx 5\,\mathrm{GeV/c^2}$ is very small.

An advantage of this technique is that it measures the top quark mass in units of m_W, which is independently known [7]. Because a dimensionless ratio is measured, the result for m_t is insensitive to any constant overall scale factor in the energy measurements.

For comparison with the results of Sect. II, the mass distribution obtained using this jet angle method are plotted as the *dot-dash curve* in Fig. 2, by scaling with the value of m_W assumed in the simulation. *The mass distribution is narrower than the best previous result by about* 6%. In addition to improved mass resolution, the curve is seen to be nearly symmetrical, and the center of the peak is very close to the mass value $175\,\mathrm{GeV/c^2}$ assumed in the simulation. The shift in the peak value due to the non-detection of neutrinos in the jets is also somewhat smaller when the jet angle method is used.

When the simulation is repeated using $m_t = 190\,\mathrm{GeV/c^2}$, the center of the peak in m_{jjj} determined by the jet angle method again comes out within 1 GeV of the input m_t, so the good features found above are not specific to the assumed mass value. The nearly exact agreement with the input mass is of course partly accidental — *e.g.*, the output mass would shift upward by $\sim 3\,\mathrm{GeV}$ if the calorimeter were able to detect neutrinos. The important result is that the output mass is close to the input one, and tracks it proportionally.

The curve shown is for jets defined by $R = 0.7$, which is approximately optimal; but a further advantage of the jet angle method is that it is found to be less sensitive to the choice of R than is the traditional invariant mass method. Defining the jets using fixed cones in the rest frames as described in Sect. II, and then using the angle method to compute m_t/m_W also works, but not quite as well as simply using the Lego definition with $R = 0.7$.

IV. DIRECT TEST

So far, we have explicitly used the original parton momenta, which are known in the simulation program, to determine the correct assignments of the observed jets. In real life, of

course, that luxury is unavailable, so one faces a combinatoric problem in analyzing semileptonic $t\bar{t}$ events. There are 12 ways to assign 4 observed jets to the b-jet from semileptonic t decay, the b-jet from hadronic t decay, and the two jets from hadronic W decay. There may be fewer combinations to try if one or both of the b-jets has been tagged; but there may be many more, since frequently there are additional jets, *e.g.*, from initial state radiation. Hence mass histograms like Figs. 1 and 2 will be contaminated by a background from events in which the jets are misassigned.

In order to test our methods directly, the HERWIG events and calorimeter simulation described above were used without making parton level cuts, and without using any of the partonic information to determine the correct jet assignments, in the following simplified event analysis:

1. Jets with observed $E_\perp > 15\,\mathrm{GeV}$ are found using $R = 0.4$ cones in (η, ϕ) space. If fewer than 4 jets are found, the event is rejected.

2. If more than 4 jets are found, only those with the 4 largest values of $p_\perp$ are kept. We ignore b-tagging here, so all 12 ways of assigning the jets to the 4 expected jets are examined. (By trying all possible subsets of 4 jets, it would be possible to reclaim an additional $\sim 10\%$ of good events; but the combinatoric and non-top backgrounds to those events would be considerably larger, and the mass resolution not quite as good, so this will be of doubtful value even in the final data analysis.)

3. An iteration similar to that described in Sect. II is carried out, so that each calorimeter cell within $R = 0.7$ of any one of the 4 significant jet axes is associated with the nearest of those axes.

4. The transverse momentum of the neutrino is estimated as usual as the negative of the total observed $\vec{p}_\perp$. Its longitudinal momentum is estimated by requiring $m_{\ell\nu}$ to equal the W mass used in the simulation. The magnitude of the rapidity difference $|\eta_\nu - \eta_\ell|$ is then given by

$$m_{\ell\nu}^2 = 2\, p_\perp^\ell\, p_\perp^\nu\, [\cosh(\eta_\nu - \eta_\ell) - \cos(\phi_\ell - \phi_\nu)]\ . \tag{3}$$

The sign of $\eta_\ell - \eta_\nu$ is assumed to be the same as the sign of η_ℓ, which corresponds to choosing between the two possible solutions for $p_\parallel^\nu$ the one giving the smaller energy for the leptonically decaying W. If Eq. (3) has no solution (because $\cosh(\eta_\nu - \eta_\ell) < 1$), we take $\eta_\nu = \eta_\ell$ [3]; or reject the event if there is no solution with $m_{\ell\nu} < 100$.

5. We reject some candidate jet assignments immediately on the basis of very loose cuts: we require $120 < m_{b\ell\nu} < 220$ for the leptonically decaying top and $55 < m_{\rm jj} < 100$ for the hadronically decaying W. (Broad cuts on the hadronic top mass, or on the minimum non-W dijet mass in the hadronic top might also be useful at this point [3].)

6. To select the correct jet assignment according to the best fit to the leptonic top and hadronic W masses, we define a measure of fit by

$$\begin{aligned} D &= \sqrt{D_1^2 + D_2^2} \\ D_1 &= (m_{b\ell\nu}^3 - m_1^3)/(3\, m_1^2\, \Delta_1) \\ D_2 &= (m_{jj}^2 - m_2^2)/(2\, m_2\, \Delta_2)\ . \end{aligned} \tag{4}$$

The parameters $m_1 = 169$, $\Delta_1 = 16$, $m_2 = 78.3$, $\Delta_2 = 6.7$ in GeV = 1 units were found using the previous simulation, by making the range $-1.0 < D_1 < +1.0$ correspond to the middle 60% of the probability distribution for $m_{b\ell\nu}$ for the correct jet assignment, while $-1.0 < D_2 < +1.0$ corresponds similarly to the middle 60% of the $m_{\rm jj}$ distribution for W decay. The cubic ($m_{b\ell\nu}^3$) and quadratic (m_{jj}^2) forms in Eq. (4) were chosen because these quantities have more symmetrical probability distributions than the QCD-skewed masses themselves. The factors in the denominators were chosen to make the constants Δ_1 and Δ_2 correspond directly to the widths of the distributions.

When it comes time to analyze real data, the parameters in Eq. (4) can be tuned using Monte Carlo events. Also, the parameters in D_1 should be adjusted to be self-consistent with m_t as measured by the hadronic t decays. Actually, the analysis could

no doubt be improved by allowing for differences in the expected range for the observed $m_{b\ell\nu}$, based on the configuration of ℓ and ν momenta. Additional contributions to the measure of fit for each possible jet assignment could also be included, *e.g.*, based upon the transverse and longitudinal momenta of the t and $\bar{t}$.

7. The jet assignment that gives the lowest value of D is assumed to be the correct one. A small number of events (8%) with a poor fit ($D > 2.5$) are rejected. A further 17% of events are rejected when any two of the four final jet axes are separated by less than 0.7 in Lego. Otherwise, the corresponding mass for $t \to \mathrm{jjj}$ is entered into a histogram to create Fig. 3.

Note that we adopt the idea advocated in Ref. [3] that the t mass measurement should be based on the hadronically decaying top. The mass of the leptonically decaying one contributes only to choosing the correct set of jet assignments. This avoids a number of possibilities for systematic errors due to uncertainties in the neutrino momentum measurement. Only the central value assumed for the leptonic decay mass needs to be tuned to match the final average m_t found in the experiment. If the assumed value is incorrect, it will reduce the signal rate, but should not change the measured hadronic top mass.

Fig. 3 shows the m_{jjj} distributions for $t \to bW \to \mathrm{jjj}$. The *dotted curve* shows the invariant mass given by the original $R = 0.4$ cones. The *solid curve* shows the invariant mass given by $R = 0.7$ cones, including the iteration that assigns calorimeter cells to the nearest decay jet axis. Note that going from $R = 0.4$ to $R = 0.7$ yields a dramatic improvement in the sharpness of the peak, and considerably reduces the downward shift in mass relative to the $m_t = 175$ input to the simulation. The benefits of going to $R = 0.7$ cones is actually even greater than what is shown here, because the larger cones were used to infer the correct jet assignments for both curves.

The *dot-dashed curve* shows the result of calculating m_{jjj} by the jet angle method of Sect. III. It shows a clear peak that is more symmetrical and is centered closer to the input value of m_t, confirming the results of Sect. III. The peak is not quite as high as the $R = 0.7$ result,

which may be due to the fact that the ordinary cone method is somewhat less affected by misassigned jets, since the value it gives for $m_{\rm jjj}$ is independent of which of the three dijet pairs is identified as the hadronically decaying W.

The jet angle method and the ordinary invariant mass offer two largely independent measurements of $m_{\rm jjj}$ in each event. We can combine the two measurements to obtain an average that has smaller errors than either measurement by itself. To allow for the fact that the two measurements contain different systematic mass shifts, it is seems appropriate to combine them by taking their geometric mean $m_{\rm ave} = \sqrt{m_{\rm jjj}^{(1)}\, m_{\rm jjj}^{(2)}}$, although the distribution of their simple average is almost identical. The resulting mass histogram, shown as the *dashed curve* in Fig. 3, displays the best peak of all. This mass variable is therefore most promising for future analyses of $t\bar{t}$ data.

V. CONCLUSIONS

In summary, we have seen that

1. To obtain the best mass resolution for hadronic top decays, it is essential to use a sufficiently large cone size $R \simeq 0.7$ in the Lego variables $(\eta,\ \phi)$ of the detector, and to include an iteration whereby final particles within each of the four jet cones $\sqrt{(\Delta\eta)^2 + (\Delta\phi)^2} < R$ of the $t\bar{t}$ final state are self-consistently assigned to the nearest axis. Quantitatively, going from $R = 0.3$ to $R = 0.5$ reduces the width of the top mass peak by a factor ≈ 0.80. Going on from $R = 0.5$ to $R = 0.7$ reduces it by a further factor ≈ 0.86.

2. A suggestion to define the jets by cones of fixed angle in the rest frames of the decaying t and W was argued to be plausible and shown to be simple to carry out, but did not in fact improve the mass resolution. Instead, it gave results similar to $R = 0.7$.

3. A suggestion to compute the top mass in each event on the basis of the jet angles in the measured t rest frame, using the zero-mass kinematical formula Eq. (2), was shown

to make a significant improvement in the measurement of m_t. It reduces the width of the top mass peak slightly, and makes the peak more symmetrical and less sensitive to the choice of R. This jet angle method is very easy to apply, since the necessary angles are easily computed from the jet four-momentum estimates using Eq. (1). A further advantage of this method is that it measures m_t as a ratio to the known m_W, and is thus insensitive to the absolute calibration for jet energy measurements.

4. An even better measure of m_t in each event can be obtained using the geometric mean $m_{\rm ave} = \sqrt{m_{\rm jjj}^{(1)}\, m_{\rm jjj}^{(2)}}$ of the two measures of $m_{\rm jjj}$ given by the ordinary Lorentz-invariant mass of the three-jet system, and the jet angle method.

These conclusions have been confirmed by the simulation of Sect. IV, which is a simplified version of the essence of actual $t\bar{t}$ data analysis.

To clarify the point regarding cone size, let us examine the standard experimental practice of "correcting" the jet $p_\perp$ measured in a small cone, by a factor that is determined from Monte Carlo simulation, or experimentally, *e.g.*, by studying the $p_\perp$ balance of hard scattering in events with a direct photon and a jet. This correction factor could in general be a function of $p_\perp$ and η. However, no such "out-of-cone correction" can improve the trijet mass resolution on a par with actually *using* larger cones, since when the latter is done, the revisions in $p_\perp$ are found to vary widely from case to case as a direct result of the QCD collinear radiation singularity. This is shown in Fig. 4, which displays the distribution of jet transverse energy increases in going from $R = 0.4$ to $R = 0.7$ in the simulation of Sect. IV, for jets from events in the signal peak with a typical $p_\perp \approx 40$ in the smaller cones. Quantitatively, the middle 68% of the probability distribution extends from 1.0 to 6.7 for the b-jets, and from 0.8 to 5.8 for the jets from W decay.

The importance of ample cone size, with final state energies assigned to the nearest cone, has been clearly demonstrated. The jet angle method has been shown to have significant advantages. Although the rest-frame cone method was found to be no better than the standard procedure, it should still be pursued on the grounds that its systematic errors

might be different from the conventional analysis.

Most importantly, the mass variable $m_{\rm ave}$, defined as the geometric mean of the two estimates of m_t using $R = 0.7$ cones, should be tried since it produced the best mass resolution of all methods examined here. The improved resolution should help to reduce the statistical uncertainty in the location of the mass peak, which will arise from the rather small number of events (~ 100) expected in each experiment by the end of the current Tevatron running period. This technique should therefore improve the accuracy of the top quark mass measurement.

The next steps, which can only be carried out by the experimenters of CDF and DØ, must be to try these procedures using full detector simulations, and then real data.

The improvements in mass resolution could also help with the the difficult problem of observing doubly hadronic top events $t\bar{t} \to (W b)\,(W\,b) \to 6\,\text{jets}$ [10].

ACKNOWLEDGMENTS

I thank S. Kuhlmann, J. Huston, J. Linnemann, T. Ferbel, and S. Snyder for information about the experiments. This work was supported in part by U.S. National Science Foundation grant number PHY-9507683.

REFERENCES

[1] CDF Collaboration (F. Abe *et al.*), Phys. Rev. Lett. **74**, 2626 (1995).

[2] DØ Collaboration (S. Abachi *et al.*), Phys. Rev. Lett. **74**, 2632 (1995).

[3] P. Agrawal, D. Bowser-Chao, and J. Pumplin, "Optimized Top Quark Analysis with the Decision Tree" (hep-ph/9503453), submitted to Phys. Rev. D.

[4] G. Abbiendi, I.G. Knowles, G. Marchesini, B.R. Webber, M.H. Seymour and L. Stanco, Comp. Phys. Comm. **67**, 465 (1992).

[5] OPAL Collaboration (R. Akers *et al.*), Z. Phys. **C63**, 181 (1994).

[6] OPAL Collaboration (R. Akers *et al.*), Z. Phys. **C63**, 197 (1994).

[7] CDF Collaboration (F. Abe *et al.*), Phys. Rev. Lett. **75**, 11 (1995).

[8] J. Pumplin, Phys. Rev. **D45**, 806 (1992).

[9] J. Pumplin, Phys. Rev. **D44**, 2025 (1991).

[10] W. T. Giele *et al.*, Phys. Rev. **D48**, 5226 (1993).

FIGURES

FIG. 1. Simulated dijet invariant mass distribution for $W \to \mathrm{jj}$ from semileptonic top events. The *dotted* curve is for jets defined by $\sqrt{(\Delta\eta)^2 + (\Delta\phi)^2} < 0.3$ cones in the rest frame of the detector. The *solid* curve is for jets defined by $\sqrt{(\Delta\eta)^2 + (\Delta\phi)^2} < 0.7$ cones in the rest frame of the detector. The *dashed* curve is for jets defined by $\theta < 45^\circ$ cones in the W rest frame, via the iteration proposed in Sect. II. A heavy tick mark indicates the value of m_W assumed in the simulation.

FIG. 2. Simulated trijet invariant mass distribution for $t \to W\,b \to \mathrm{jjj}$ from semileptonic top events. As in Fig. 1, the *dotted* curve is for jets defined by $\sqrt{(\Delta\eta)^2 + (\Delta\phi)^2} < 0.3$ cones, the *solid* curve is for $\sqrt{(\Delta\eta)^2 + (\Delta\phi)^2} < 0.7$ cones, and the *dashed* curve is for $\theta < 45^\circ$ cones in the t rest frame for the b-jet and in the W rest frame for the other two. The *dot-dashed* curve is for $\sqrt{(\Delta\eta)^2 + (\Delta\phi)^2} < 0.7$ cones with m_{jjj} computed by the "jet angle method" of Sect. III. A heavy tick mark indicates the value of m_t assumed in the simulation.

FIG. 3. Trijet invariant mass distribution for $t \to Wb \to \mathrm{jjj}$ from the more complete simulation of Sect. IV. The *dotted* curve is for jets defined by $R = 0.4$ cones. The *solid* curve is for jets defined by $R = 0.7$ cones. The *dot-dashed* curve is for the same $R = 0.7$ cones, with m_{jjj} computed by the "jet angle method" of Sect. III. The *dashed* curve, which gives the best resolution of all, is for the same $R = 0.7$ cones, with m_{jjj} computed as the geometric mean of the two previous mass measures.

FIG. 4. The increase in jet $p_\perp$ when the cone size is increased from $R = 0.4$ to $R = 0.7$ for jets that contribute to the signal peak $155 < m_{\mathrm{ave}} < 185$, with $p_\perp \approx 40$ in the smaller cones. *Solid* curve = b-jets from leptonic top decay, *dashed* curve = b-jets from hadronic top decay, and *dotted* curve = jets from hadronic W decay are all about the same. The large range of the distribution directly shows the importance of using the larger cones to analyze each jet, rather than attempting to make do with smaller cones and compensating by an average "out-of-cone correction."

FIG. 1

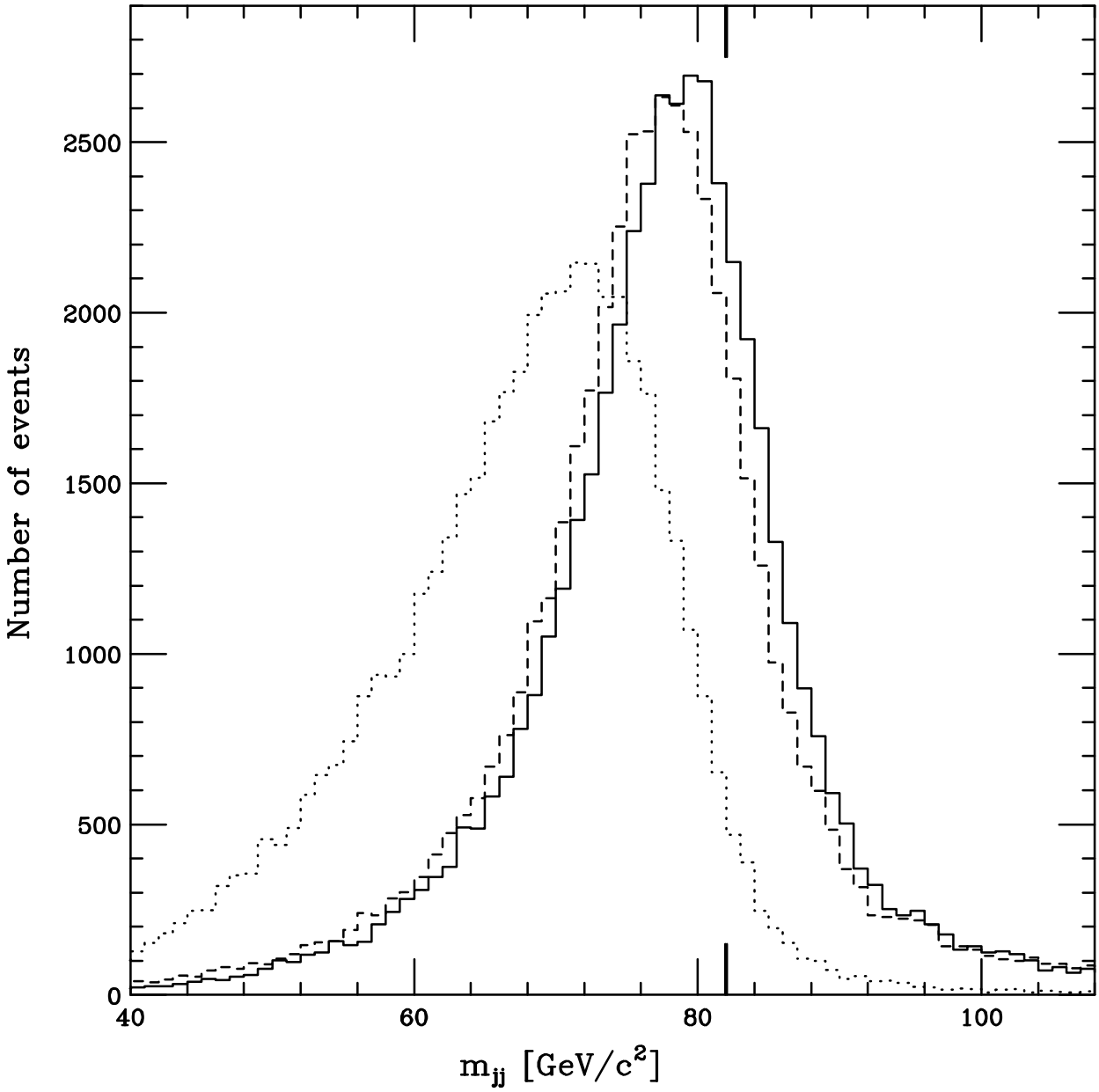
Number of events
0
500
1000
1500
2000
2500
40
60
80
100
m_{jj} [GeV/c^2]

FIG. 2

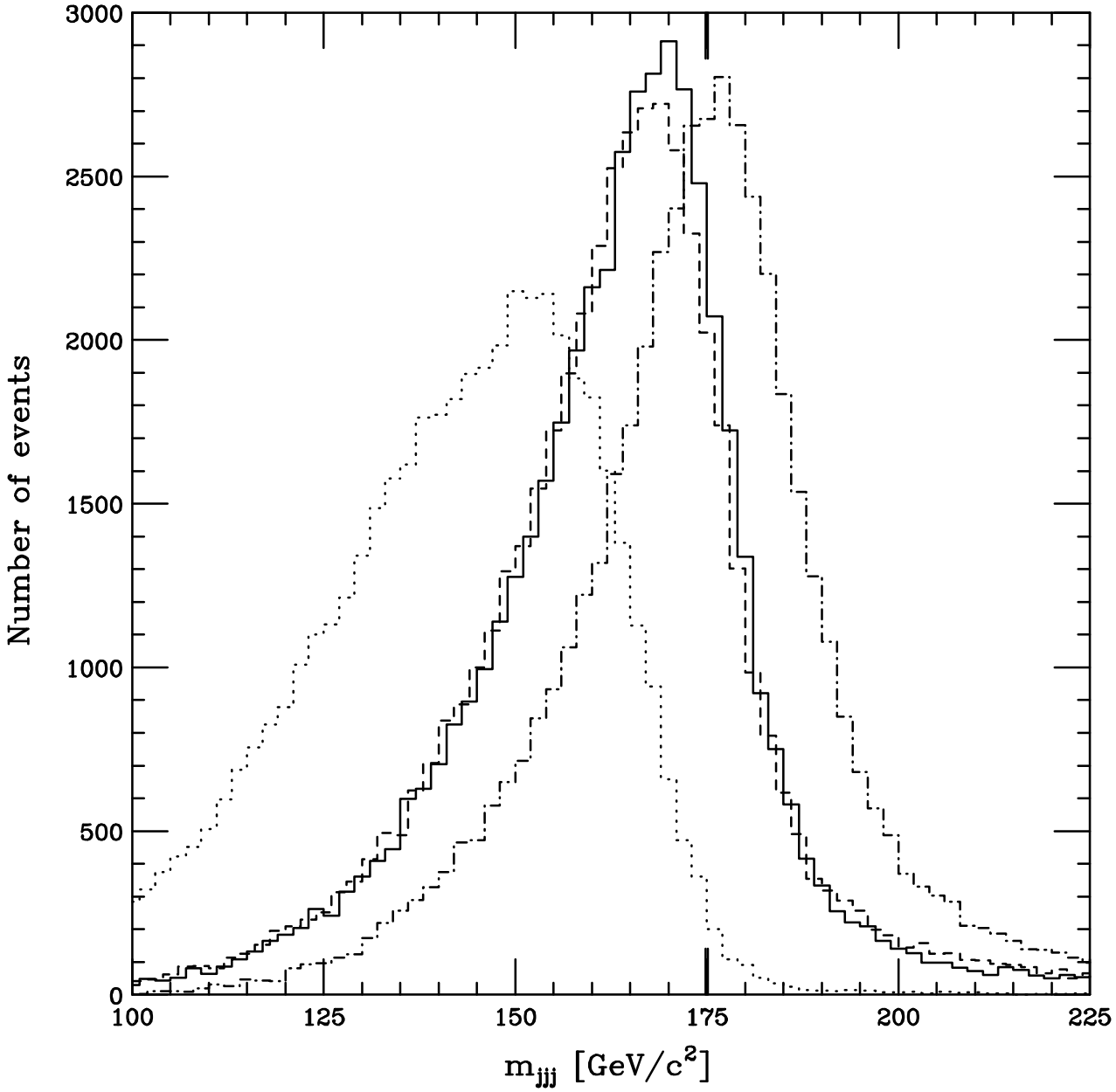
3000
2500
2000
1500
1000
500
0
Number of events
100
125
150
175
200
225
m_{jjj} [GeV/c^2]

FIG. 3

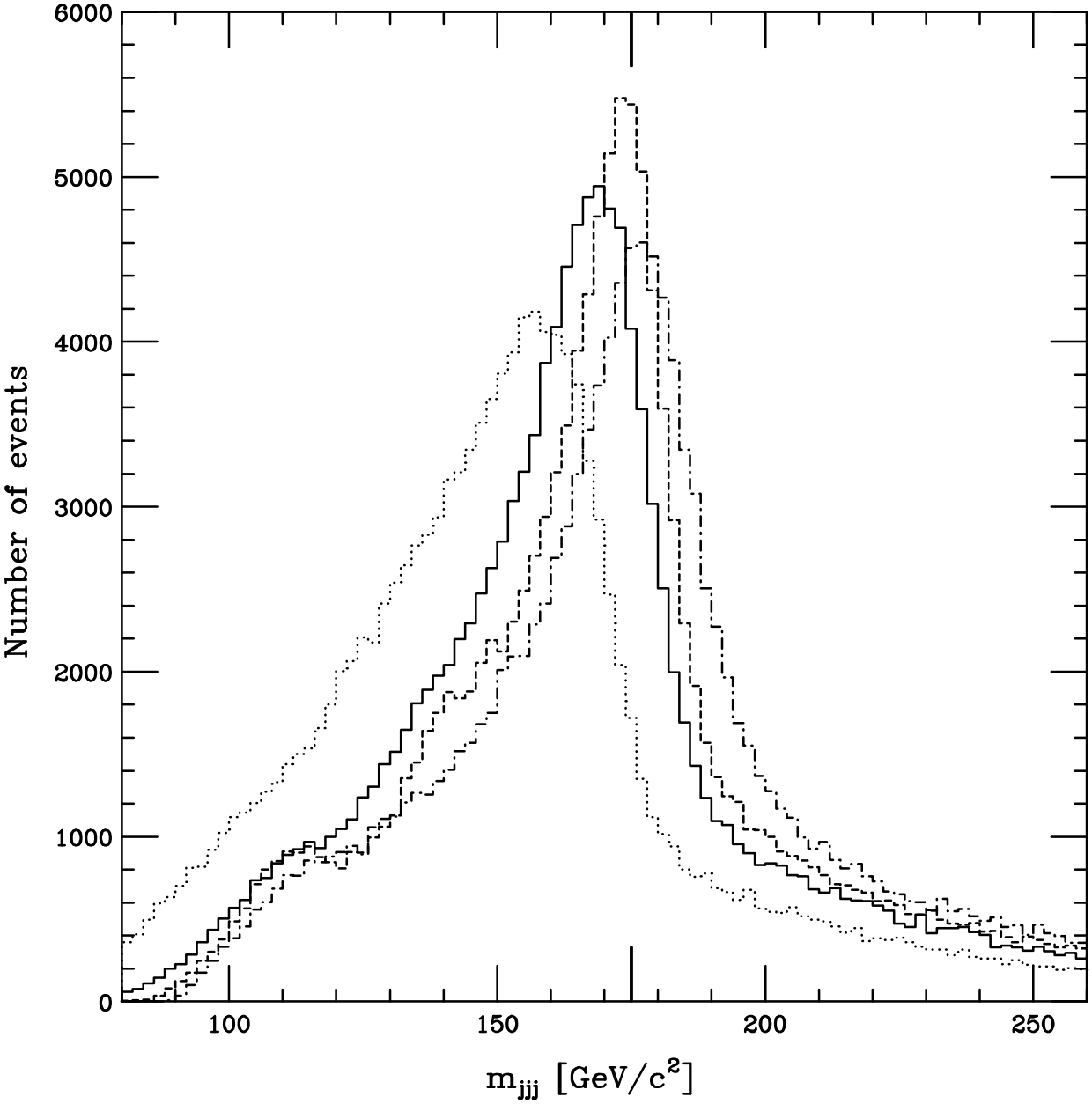
6000
5000
4000
3000
2000
1000
0
Number of events
100
150
200
250
m_{jjj} [GeV/c^2]

FIG. 4

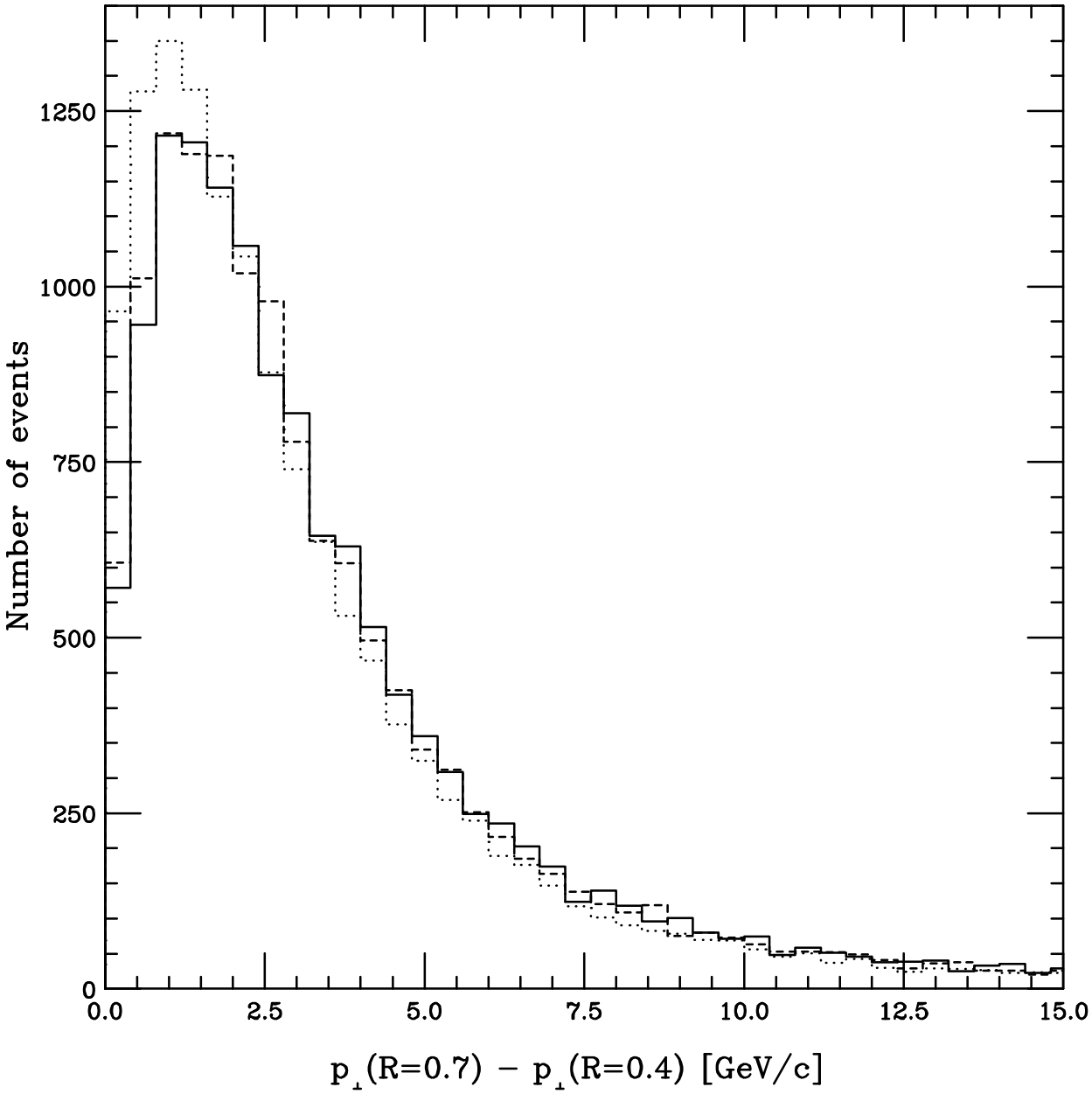
Number of events
1250
1000
750
500
250
0
0.0
2.5
5.0
7.5
10.0
12.5
15.0
p⊥(R=0.7) − p⊥(R=0.4) [GeV/c]